Mutant MFN2/*fzo-1* selectively removes mitochondrial DNA heteroplasmy in *Caenorhabditis elegans* and in Charcot-Marie-Tooth patients

Lana Meshnik[1], Dan Bar-Yaacov[1], Dana Kasztan[1], Tal Cohen[1], Mor Kishner[1], Itay Valenci[1], Sara Dadon[1], Christopher J. Klein[2], Jeffery M. Vance[3], Yoram Nevo[4], Stephan Zuchner[3], Dan Mishmar[1,*] and Anat Ben-Zvi[1,*]

[1] Department of Life Sciences, Ben-Gurion University of the Negev, Beer Sheva, Israel

[2] Department of Neurology, Division of Neuromuscular Medicine, Mayo Clinic, Rochester, MN, USA

[3] Dr. John T. Macdonald Foundation Department of Human Genetics and Hussman institute for Human Genomics, Miller School of Medicine, University of Miami, Miami, FL, USA

[4] Neurology Institute, Schneider Children's Medical Center of Israel, Tel-Aviv University, Petach Tikva, Israel

* Corresponding authors

Prof. Anat Ben-Zvi

Tel: +972-8-6479059

Fax: +972-8-6479041

E-mail: anatbz@bgu.ac.il

Prof. Dan Mishmar

Tel: +972-8-6461355

Fax: +972-8-6461356

E-mail: dmishmar@bgu.ac.il

Abstract

Deleterious and intact mitochondrial DNA (mtDNA) mutations frequently co-exist in cells (heteroplasmy). Such mutations likely survive and are inherited due to complementation via the intra-cellular mitochondrial network. Hence, we hypothesized that compromised mitochondrial fusion would hamper such complementation, thereby affecting heteroplasmy inheritance. To test this hypothesis, we assessed heteroplasmic patterns in three Charcot-Marie-Tooth disease type 2A pedigrees, which carry a mutated mitofusin 2 (MFN2). We found reduced prevalence of a potentially functional mtDNA heteroplasmic mutation in these patients, as compared to healthy maternal relatives, while neutral heteroplasmic mutations fluctuated randomly. Secondly, we found that MFN2 dysfunction in a *Caenorhabditis elegans* model carrying a large heteroplasmic mtDNA deletion (ΔmtDNA) led to a severe developmental delay and embryonic lethality. Strikingly, these phenotypes were relieved during subsequent generations in association with complete ΔmtDNA removal. Such ΔmtDNA loss occurred during both gametogenesis and embryogenesis. Therefore, mitochondrial fusion is essential for inheritance of mtDNA heteroplasmy.

Key words: *C. elegans*, Charcot-Marie-Tooth disease, heteroplasmy, mitofusine 2, mtDNA,

Introduction

Unlike the nuclear genome, mitochondrial DNA (mtDNA) is present in multiple copies per animal cell. For instance, human somatic cells contain an average of ~1,000 mitochondria per cell, with each mitochondrion harboring 1-10 mtDNA copies (Schon and Gilkerson, 2010). Although this large intracellular mtDNA population is inherited from the maternal germline, and hence carries a single major haplotype, mtDNA molecules can differ in sequence (heteroplasmy) either due to inheritance of mutations from the ovum or due to the accumulation of changes over the lifetime of the individual (Avital et al., 2012). Some of these changes may have pathological consequences, as reflected in a variety of mitochondrial disorders, yet only upon crossing a threshold of prevalence in the cell (Hahn and Zuryn, 2019). Accordingly, the penetrance of disease-causing mutations ranges between 60-80%, depending on the symptoms and tissues that display the specific phenotype (Craven et al., 2017).

The repertoire of heteroplasmic mutations varies among cells and tissues of an individual, mainly due to replicative segregation (drift) of the mitochondria during cell division and mitochondrial bottlenecks that appear during embryo development (Floros et al., 2018). However, it has been suggested that heteroplasmy can be modulated by non-random factors, including selection (Avital et al., 2012; Burgstaller et al., 2014). Indeed, it has been shown that mitophagy, a mechanism of mitochondrial quality control, partially provides selection against defective mitochondria and maintains disease-causing mtDNAs below the threshold level both in human cells (Suen et al., 2010) and in a *Caenorhabditis elegans* model (Valenci et al., 2015). Mitophagy requires proper fission-fusion cycles of the mitochondrial network so as to allow removal of dysfunctional mitochondria (Mao et al., 2013; Twig et al., 2008). In agreement with this notion, reduction in heteroplasmy levels of potentially deleterious mtDNA mutations was observed when components of the fusion machinery were compromised in *Drosophila* models (Kandul et al., 2016). Furthermore, elevated heteroplasmy levels of pathological mtDNA were observed when the fission machinery was disrupted in cell culture (Malena et al., 2009). This suggest that the effect of disease-causing mutations is functionally compensated at sub-threshold levels of heteroplasmy by the intracellular mitochondrial network (Busch et al., 2014; Hahn and Zuryn, 2019; Schon and Gilkerson, 2010). This offers an appealing explanation for the relatively high abundance of low-level disease-causing heteroplasmic mutations in the general population (Rebolledo-Jaramillo et al., 2014; Ye et al., 2014). We thus hypothesized that interfering with the mitochondrial cellular network would prevent functional compensation of heteroplasmic mutations, and potentially lead to their removal.

This question is of special interest in the case of human disorders in which the fusion machinery is compromised. A good example for such, is the mutated mitochondrial fusion protein MFN2, leading to the hereditary motor and sensory neuropathy Charcot-Marie-Tooth type 2A (CMT2A), which is characterized by progressive loss of muscle mass across the entire human body, and primary axonal neuropathies (Zuchner et al., 2004).

Here, we took the first steps towards testing this hypothesis by assessing patterns of mtDNA heteroplasmy in three unrelated CMT2A pedigrees. In doing so, we found significantly reduced heteroplasmy levels only in patients carrying a potentially functional heteroplasmic mutation. Secondly, crossing *C. elegans* harboring a MFN (*fzo-1*) deletion to animals carrying a large heteroplasmic mtDNA deletion resulted in a developmental delay and embryonic lethality, which was alleviated in subsequent generations concomitant with a complete loss of the truncated mtDNA molecules. The mechanistic implications of these findings are discussed.

Results

MFN2 modulates heteroplasmic patterns in CMT2A patients: To assess the potential impact of defective MFN2 on the dynamics of mitochondrial heteroplasmy in humans, we employed massive parallel sequencing (MPS) of the entire mtDNA in CMT2A patients and healthy maternal relatives in three independent pedigrees (Fig. S1). High coverage per mtDNA nucleotide (>1000X) was attained at a mean of 16560 mtDNA positions, thus allowing both assignment of samples to specific mtDNA genetic backgrounds (haplogroups) and the detection of heteroplasmy levels >1% (Table S1).

In pedigree 1, a Caucasian-Cherokee American Indian family in which a Leu146Phe MFN2 mutation (Klein et al., 2011) has been segregating, five heteroplasmic mutations were identified, two of which (mtDNA positions 310 and 16172) are shared between the female patient (sample V17) and her healthy siblings (samples V13 and V14; Table 1). Interestingly, although the C-to-G transition at position 16172 was highly prevalent (~95%) in the healthy maternal siblings, it became rare in the patient (~5%). Notably, position 16172 maps within the mtDNA transcription termination site (TAS) (Barshad et al., 2018), thus suggesting potential functionality. In pedigree 2 (Caucasian family 1706, with the L76P MFN2 mutation (Zuchner et al., 2004)), a heteroplasmic transition at mtDNA position 13830 was identified (a synonymous mutation in the ND5 gene), which differentially segregated among patients and healthy maternal relatives. Nevertheless, the ratio between the two segregating alleles at this position was the opposite of what was seen between the proband (individual 106) and his maternal uncle, who was also a patient

(individual 1007). This finding is consistent with random segregation of this heteroplasmic mutation. Finally, analysis of the entire mtDNA sequence in patients and healthy maternal relatives in pedigree 3 (an Arab-Israeli family presenting the Q386P MFN2 mutation (Verhoeven et al., 2006)) did not reveal any trustworthy heteroplasmic mutations. Thus, we found that only in the case where a heteroplasmic mutation was potentially functional was its level significantly declined exclusively in the CMT2A patient, suggesting that selective heteroplasmy removal had occurred. As such, we hypothesized that MFN2 likely modulates the inheritance of functional heteroplasmic mutations. To test this proposal, we examined the dynamics of a previously characterized heteroplasmic mtDNA deletion (Gitschlag et al., 2016; Liau et al., 2007; Tsang and Lemire, 2002) in an MFN2 *C. elegans* mutant.

A heteroplasmic deletion cannot be tolerated in a *C. elegans* mitofusin (*fzo-1*) mutant: The stable heteroplasmic *C. elegans* strain *uaDf5/+* harbors a mixture of intact (+mtDNA) and ~60% of a 3.1 kb mtDNA deletion (ΔmtDNA) (Gitschlag et al., 2016; Tsang and Lemire, 2002). Although lacking four essential genes (i.e., mt-ND1, mt-ATP6, mt-ND2 and mt-Cytb), this strain displays only mild mitochondrial dysfunction (Gitschlag et al., 2016; Liau et al., 2007; Tsang and Lemire, 2002). We showed that dysfunctional PDR-1, the worm orthologue of the key mitophagy factor Parkin, led to elevated levels of the truncated mtDNA, suggesting that mitochondrial quality control senses the presence of dysfunctional mitochondria (Valenci et al., 2015). In conjunction with this finding, RNAi knockdown of *fzo-1,* the *C. elegans* orthologue of MFN1/2*,* led to slight reduction in the levels of the heteroplasmic ΔmtDNA, although without any phenotypic consequences (Nargund et al., 2012). We, therefore, asked what would be the impact of the *fzo-1(tm1133)* deletion (hereafter designated as *fzo-1(mut)*) on the inheritance of the maternal ΔmtDNA.

To this end, we crossed ΔmtDNA heteroplasmic hermaphrodites with *fzo-1(mut)* heterozygote males (Fig. 1A). After self-cross of the F1 progeny, the distribution of the genotypes in the F2 heteroplasmic progeny did not deviate from the expected Mendelian ratios, namely 26% homozygous *fzo-1(mut)*, 49% *fzo-1* heterozygotes (*ht*) and 25% *fzo-1(wt)* (p=0.94, Chi square test; Table S2). No apparent phenotypic differences were observed among F2 animals (generation 1, G1) as well as in the non-heteroplasmic *fzo-1(mut)* animals. However, we noticed that only 13±5% of the second generation (G2m; i.e., the progeny of the self-crossed *fzo-1(mut);*ΔmtDNA worms) hatched, as compared to *fzo-1(mut)* animals (67±5%; Fig. 1B). Interestingly, the 13±5% G2m animals that did hatch

were developmentally delayed, and no animals reached adulthood after six days. This was in contrast to ~75% of the G1 animals that reached adulthood (Fig. 1C). These findings demonstrate that the interaction between the heteroplasmic ΔmtDNA and the nuclear DNA-encoded *fzo-1* mutant led to a severe reduction in fitness. Therefore, the ΔmtDNA was not tolerated by mitofusin mutants.

Reversal of the adverse effects of the ΔmtDNA-*fzo-1* interaction: To better characterize the phenotypic impact of interactions between ΔmtDNA and *fzo-1(mut)*, we monitored the progeny of the self-crossed *fzo-1(ht);*ΔmtDNA worms. Specifically, we measured the duration of the larva-to-adulthood period during the course of development in the G1m-G4m generations (Fig. 1D). While ~75% of the G1m generation reached adulthood after six days, the development of G2m animals was severely delayed, with 75% of the animals reaching adulthood only after nine days. To our surprise, the G3m animals showed significant improvement, with ~60% of this population reaching adulthood after six days. Moreover, G4m animals showed a full reversal of ΔmtDNA-associated adverse effects (Fig. 1D). Thus, the adverse effects of the interaction between *fzo-1(mut)* and ΔmtDNA were reversed by the G4m generation.

We noted a similar pattern across generations when hatching was considered. In contrast to the ~10% hatching seen among G2m embryos, 60±8% of the G3m embryos hatched. Strikingly, the hatching percentage of the G4m generation was indistinguishable from that of G1 animals and remained stable over subsequent generations (Fig. 1B). Finally, no phenotypic changes were observed across the G1-G4 generations while tracing the developmental pace and hatching percentage of *fzo-1(wt)*;ΔmtDNA, G1wt-G4wt (Fig. S2). Taken together, our findings demonstrate a full reversal of the adverse effects of the interaction between the ΔmtDNA and the nuclear DNA-encoded mutant *fzo-1* gene.

MFN2 mutant selects against a large heteroplasmic truncation in *C. elegans*: We next asked how the deleterious interactions between *fzo-1(mut)* and ΔmtDNA were abrogated. We hypothesized that if the ΔmtDNA is not tolerated in the background of *fzo-1(mut)*, then selection against the ΔmtDNA should occur. To test this prediction, we quantified the levels of ΔmtDNA by quantitative PCR (qPCR) across the G1m-G4m generations (at the adult stage) in both the *fzo-1(mut);*ΔmtDNA and the *fzo-1(wt);*ΔmtDNA strains. We found that ΔmtDNA levels declined two-fold in the G1m *fzo-1(mut)* animals, as compared to *fzo-1* heterozygotes. This trend was enhanced, reaching a 10-fold reduction in ΔmtDNA levels in G2m animals. Values were below detection levels in most G3m

(N=19/22) and all G4m (N=21) animals (Fig. 2A). In contrast, ΔmtDNA levels did not significantly change across the G1wt-G4wt generations of *fzo-1(wt);*ΔmtDNA animals (Fig. 2B).

These results suggest that the ΔmtDNA was completely lost during the G1m-G4m generations. To test this hypothesis, we crossed G4m hermaphrodites with wild type males to isolate *fzo-1(wt)* progeny (G6). Since G6 animals (and subsequent generations) did not display any ΔmtDNA (Fig. 2A and 2C), we concluded that disrupting *fzo-1* function indeed resulted in a complete and specific loss of the deleterious heteroplasmic ΔmtDNA. Taken together, our results demonstrate, for the first time, that mitochondrial fusion is critical for maintaining heteroplasmic mutations.

ΔmtDNA levels are selected at two different stages in the *C. elegans* life cycle: We next asked at which point during the *C. elegans* life cycle was selection against ΔmtDNA realized. It was previously demonstrated that *C. elegans* mtDNA copy numbers started to increase significantly at the fourth larval stage (L4) and that this increase was associated with oocyte production (Bratic et al., 2009; Tsang and Lemire, 2002). Notably, the relative levels of ΔmtDNA are maintained during development (Tsang and Lemire, 2002). We, therefore, compared relative ΔmtDNA levels between embryos and adults in G2m animals. Our results indicate that relative ΔmtDNA levels were dramatically reduced (~5-fold) during development of G2m animals but not in G2wt animals (Fig. 3A and 3B). This observation suggests that ΔmtDNA is most likely selected against during worm development. Secondly, ΔmtDNA levels became undetectable in the resultant embryos of G2m animals (i.e., in G3m animals; Fig. 3A). Hence, it is possible that selection against ΔmtDNA molecules had already occurred during gametogenesis. In support of this claim, we noted that upon isolation of the gonads of G2m animals and then comparing ΔmtDNA levels in gonads and somatic tissues, we found a two-fold decrease in ΔmtDNA levels in the gonads. In contrast, no such difference was observed when comparing gonads and somatic tissues of *fzo-1(wt)*/ΔmtDNA animals (Fig. 3C). Based on these observations, we suggest that selection against ΔmtDNA molecules occurs both during development and during gametogenesis.

Discussion

Cell culture experiments revealed that a mixture of mtDNA molecules differing in sequence in the same cell can complement each other by the diffusion of products via the mitochondrial network, which in turn leads to a restoration of mitochondrial function

(Gilkerson et al., 2008; Schon and Gilkerson, 2010). This very same mechanism offers an explanation for the survival of mtDNA disease-causing mutations in cells and in turn, their transmission to the next generation. Therefore, we hypothesized that interfering with the intracellular mitochondrial network by compromising the fission-fusion cycle would hamper mitochondrial functional complementation.

As a first step in testing this hypothesis, we investigated patterns of mtDNA heteroplasmy in three independent pedigrees of Charcot-Marie-Tooth type 2A characterized by mutated MFN2, a major mitochondrial fusion component. We found that the heteroplasmy level of a potentially functional mutation in the mtDNA transcriptional-associated sequence was strongly reduced in patients, as compared to healthy maternal relatives. In contrast, the levels of apparently neutral mtDNA mutations fluctuated without any clear correlation to phenotype. Although offering support to our working hypothesis, the impact of a compromised fusion machinery on heteroplasmy required assessment in a more controlled system. Thus, we turned to a well-characterized *C. elegans* heteroplasmic ΔmtDNA model (Tsang and Lemire, 2002) into which we introduced a mutation in MFN2 (*fzo-1*) (Kanazawa et al., 2008). We found that *fzo-1* mutant worms experienced significant developmental delays and high rates of embryonic lethality, which were relieved within two generations. Strikingly, this improvement was accompanied by complete and selective removal of the ΔmtDNA molecules (Fig. 4). These observations strongly argue for the essentiality of a functional intracellular mitochondrial network for the survival of potentially deleterious heteroplasmic deletions.

Our findings provide experimental support for the hypothesis that functional complementation among mitochondria in the intracellular network likely enables the survival and prevalence of deleterious heteroplasmic mtDNA mutations in the population (Rebolledo-Jaramillo et al., 2014; Ye et al., 2014). However, in contrast to our findings, either *in vitro* loss of mitochondrial fusion or *in vivo* conditional deletion of both MFN1 and MFN2 in mouse skeletal muscle led to a strong reduction in mtDNA levels, which was accompanied by the accumulation of mtDNA point mutations and deletions (Chen et al., 2007; Chen et al., 2010). This apparent contradiction could stem from the different outcome of manipulating the fusion machinery in the germ line (our study) versus somatic cells. We thus argue that unlike what occurs with somatic cells, manipulating fusion in the germline leads to strong negative selection against deleterious mtDNA mutations. Hence, the complete loss of ΔmtDNA across *C. elegans* generations suggests that the fusion machinery represents an attractive candidate target for future treatment of mitochondrial disorders. Furthermore, partial inhibition of the fusion machinery might offer a safer route

to selectively remove disease-causing heteroplasmic mutations. Consistent with this suggestion, it has been demonstrated that knock-down of mitochondrial fusion components in both flies and worms reduced the levels of heteroplasmic deleterious mutations (Kandul et al., 2016; Nargund et al., 2012). While such a course of action may not completely remove the deleterious heteroplasmic mutation, selective reduction in heteroplasmy level below the functional threshold in cells could provide an attractive therapeutic approach (Bacman et al., 2018; Gammage et al., 2018).

Our results indicate that there are two stages during the nematode life cycle in which ΔmtDNA was lost, i.e., during the transition from larva to adult, and during embryogenesis. The relative decline of ΔmtDNA levels during late larval stages occurred concomitantly with mtDNA replication, which is part of gametogenesis (Ahier et al., 2018; Bratic et al., 2009). Close inspection of the data revealed that while intact mtDNA levels increased as expected, ΔmtDNA levels increased only some two-fold (Fig. S3B). Moreover, since ΔmtDNA levels dropped specifically in the gonad, ΔmtDNA molecules could either have been actively removed or selectively not replicated during gametogenesis. Secondly, our observed total loss of ΔmtDNA in the worm G3m generation (in contrast to its presence in the germline of the G2m generation) suggests another step of selection against ΔmtDNA during embryogenesis. Indeed, changes in mitochondrial morphology and function associated with lysosomal activation upon fertilization were demonstrated (Bohnert and Kenyon, 2017), which might also play a role in mitochondrial clearance. Taken together, our results suggest the existence of specific checkpoints of mtDNA heteroplasmy during development.

In summary, we have provided clear evidence showing that compromising the mitochondrial fusion machinery relieves the protective communal 'shelter' for deleterious heteroplasmic mutations, resulting in their complete and selective removal. The occurrence of such a process during embryogenesis and gametogenesis further underlines the importance of fission-fusion cycles in maintaining the integrity of mtDNA during transmission from generation to generation. Since reduced expression of MFN2 is frequently observed in the placenta after miscarriages of unexplained etiology (Pang et al., 2013), one can speculate that the combination of mtDNA disease-causing hetereoplasmic mutations along with MFN2 dysfunction is negatively selected. Finally, our findings may offer previously overlooked avenues to actively reduce levels of mtDNA heteroplasmy as an approach to treat mitochondrial disorders.

Materials and methods

Human DNA samples: Patients diagnosed with Charcot-Marie-Tooth type 2a (CMT2A) and healthy maternal relatives from three unrelated pedigrees were considered in the current study. Total blood DNA was extracted from available patients and healthy individuals of all three sibs. Pedigree 1, of English-native American admixed origin, harbors patients heterozygous for the dominant L146F MFN2 mutation (Klein et al., 2011). Pedigree 2, of North American Caucasian origin, harbors patients previously identified as heterozygous for the L76P MFN2 dominant mutation (Zuchner et al., 2004). In pedigree 3 of Israeli Arabian origin, the patient was identified as a compound heterozygote for A1157C and T1158G mRNA nucleotide position mutations, both leading to the recessive Q386P mutation (Verhoeven et al., 2006). In Fig. S1, arrows point to the tested individuals in each pedigree.

Massive parallel sequencing of the entire human mtDNA and bioinformatics analysis: The entire mtDNA of available patients and controls (Fig. S1) was amplified in three fragments using three sets of primers, as previously described (Avital et al., 2012). For each of the analyzed samples, the amplified fragments were mixed in equimolar ratios and sent for library construction and sequencing utilizing the Illumina MiSeq platform (Technion Genome Center, Israel). Paired-end reads were trimmed using TrimGalore (version 0.4.5)) F., 2015(and then mapped to the mtDNA reference sequence (rCRS) using BWA mem (version 0.7.16) with default parameters (Li and Durbin, 2009). Alignment files (SAM format) were compressed to their binary form (BAM format) using SAMtools (version 1.3) with default parameters [view –hb] and sorted using the [sort] function (Li et al., 2009). True heteroplasmic mutations were annotated using an in-house script that followed the logic of the previously established MitoBamAnnotator (Cohen et al., 2016). In brief, a pileup of the mtDNA-mapped reads was generated using the SAMtools [mpileup] function with the [-Q 30] parameter to only consider reads with a phred score higher than 30 as a measure of quality control. Next, the mapped bases were counted and the most frequent nucleotide in each mtDNA position was considered the major allele only if that nucleotide position had a minimal coverage of 10X. To avoid strand bias, the secondary mutation at a given nucleotide position was recorded only if it was represented by at least two reads per strand. mtDNA sequences were then haplotyped using HaploGrep2.0 (Kloss-Brandstatter et al., 2011).

Sanger sequencing and cloning: Sanger sequencing was employed to verify the identified heteroplasmic mutations at position 16172 (pedigree 1) and position 13830 (pedigree 2). Primers used for this amplification reactions are listed in Table S3.

NUMT exclusion: To control for possible contamination by nuclear mitochondrial DNA pseudogenes (NUMTs) in the MPS reads, mtDNA sequence contigs encompassing each of the identified mutations were BLAST screened as previously described (Blumberg et al., 2014). In brief, the highest scored nuclear DNA BLAST hits encompassing each of the identified mutations were aligned against the mtDNA sequence reads of the relevant sample and the number of reads harboring the exact identified mutation was counted using IGV viewer (Robinson et al., 2011). Notably, as the mtDNA is maternally inherited as a single locus, variants appear in linkage. Hence, combinations of variants that were present in nuclear DNA BLAST hits but which were not identified in sequence reads of the relevant samples were not considered as corresponding to NUMTs.

Nematodes and growth conditions: A list of strains used in this work and name abbreviations is found in Table S4. All strains were outcrosses to our N2 stock at least four times. Nematodes were grown on Nematode Growth Medium (NGM) plates seeded with the *Escherichia coli* OP50-1 strain at 15°C. Experiments were repeated at least three times. P values were calculated using the Wilcoxon Mann-Whitney rank sum test to compare two independent populations.

Crosses: Mutant *fzo-1(tm1133)* animals (strain CU5991) are very poor in mating and, therefore, were first crossed with males expressing a yellow fluorescent protein marker (*unc-54p::YFP*). Heteroplasmic (*uaDf5/*+) hermaphrodites were then crossed with *fzo-1(tm1133); unc-54p::YFP* heterozygote males to ensure maternal inheritance of *uaDf5* ΔmtDNA and to establish independent heteroplasmic lines carrying the wild type or *fzo-1(tm1133)* mutation. F2 progeny were screened for the *fzo-1(tm1133)* mutation using a single worm PCR Phire Animal Tissue Direct PCR Kit (Thermo Scientific) with *fzo-1* MUT primers (Table S5), followed by gel electrophoresis of the PCR products. Heteroplasmic (*uaDf5/*+) animals that were heterozygotes for *fzo-1(tm1133)* were maintained to easily produce G1 animals.

Gonad dissection: G2 wild type or mutant animals were placed in a drop of ultra-pure water on a coverslip slide and a 25 gauge needle was used to remove the gonads from

the body of the animals. 5-10 worms were used for each biological repeat. Gonads or the remaining carcasses were then transferred to DNA extraction buffer.

DNA purification and extraction: Total DNA was extracted using a QuickExtract kit (Lucigen). Unless otherwise indicated, DNA was extracted from a single worm ($n \geq 20$). When populations were examined, ~5 animals were collected. For embryos, DNA was extracted from ~30 embryos. For gonad and soma analysis, gonads were dissected from ~5 animals per biological repeat. DNA was extracted separately from the gonads and soma.

Assessment of mtDNA copy numbers: mtDNA levels were measured by qPCR performed on a C1000 Thermal Cycler (Bio-Rad) with KAPA SYBRFAST qPCR Master Mix (KAPA Biosystems). Analysis of the results was performed using CFX Manager software (Bio-Rad). To quantify the different mtDNA molecules, three set of primers were used for truncated, intact and total mtDNA molecules (Table S5). The average C_T (threshold cycle) of triplicate values obtained for these mtDNA molecules was normalized to a nuclear DNA marker using the $2^{-\Delta\Delta C_T}$ method (Livak and Schmittgen, 2001). At least four independent experiments were used to determine the normalized C_T values of each strain or generation. Truncated/total ratio was defined as the ratio of the normalized C_T values of truncated to total mtDNA for a given strain.

Embryo hatching: Gravid animals were moved to fresh plate for 2-12 hours and then removed from the plates. Embryos were allowed to develop and hatching was examined after 48 hours. Experiments were repeated independently at least four times.

Developmental timing: Single embryos were placed on fresh plates and allowed to grow at 15°C. The animals' developmental stage was examined every day and the number of animals reaching reproductive adulthood on each day was recorded. Developmentally arrested animals were excluded. Experiments were repeated independently at least three times.

Acknowledgements

This study was funded by the Israel Science Foundation (ISF) grant 278/18 to ABZ and grant 372/17 to DM and by Israel Ministry of Science and Technology grant 3-14337 to ABZ.

Author Contributions

Conceptualization, A.B. and D.M.; Methodology, L.M., D.B. and I.V.; Investigation, L.M., D.B., D.K., M.K. and S.D.; Formal Analysis, D.B and T.C; Resources, C.J.K., J.M.V., Y.N. and S.Z; Writing – Original Draft, A.B. and D.M.; Writing – Review & Editing, A.B. and D.M.; Supervision, A.B. and D.M.; Funding Acquisition, A.B. and D.M.

References

Ahier, A., Dai, C.Y., Tweedie, A., Bezawork-Geleta, A., Kirmes, I., and Zuryn, S. (2018). Affinity purification of cell-specific mitochondria from whole animals resolves patterns of genetic mosaicism. Nat Cell Biol *20*, 352-360.

Avital, G., Buchshtav, M., Zhidkov, I., Tuval Feder, J., Dadon, S., Rubin, E., Glass, D., Spector, T.D., and Mishmar, D. (2012). Mitochondrial DNA heteroplasmy in diabetes and normal adults: role of acquired and inherited mutational patterns in twins. Hum Mol Genet *21*, 4214-4224.

Bacman, S.R., Kauppila, J.H.K., Pereira, C.V., Nissanka, N., Miranda, M., Pinto, M., Williams, S.L., Larsson, N.G., Stewart, J.B., and Moraes, C.T. (2018). MitoTALEN reduces mutant mtDNA load and restores tRNA(Ala) levels in a mouse model of heteroplasmic mtDNA mutation. Nat Med *24*, 1696-1700.

Barshad, G., Marom, S., Cohen, T., and Mishmar, D. (2018). Mitochondrial DNA Transcription and Its Regulation: An Evolutionary Perspective. Trends Genet *34*, 682-692.

Blumberg, A., Sri Sailaja, B., Kundaje, A., Levin, L., Dadon, S., Shmorak, S., Shaulian, E., Meshorer, E., and Mishmar, D. (2014). Transcription factors bind negatively selected sites within human mtDNA genes. Genome Biol Evol *6*, 2634-2646.

Bohnert, K.A., and Kenyon, C. (2017). A lysosomal switch triggers proteostasis renewal in the immortal C. elegans germ lineage. Nature *551*, 629-633.

Bratic, I., Hench, J., Henriksson, J., Antebi, A., Burglin, T.R., and Trifunovic, A. (2009). Mitochondrial DNA level, but not active replicase, is essential for Caenorhabditis elegans development. Nucleic Acids Res *37*, 1817-1828.

Burgstaller, J.P., Johnston, I.G., Jones, N.S., Albrechtova, J., Kolbe, T., Vogl, C., Futschik, A., Mayrhofer, C., Klein, D., Sabitzer, S., et al. (2014). MtDNA segregation in heteroplasmic tissues is common in vivo and modulated by haplotype differences and developmental stage. Cell Rep *7*, 2031-2041.

Busch, K.B., Kowald, A., and Spelbrink, J.N. (2014). Quality matters: how does mitochondrial network dynamics and quality control impact on mtDNA integrity? Philosophical Transactions of the Royal Society B: Biological Sciences *369*, 20130442.

Chen, H., McCaffery, J.M., and Chan, D.C. (2007). Mitochondrial fusion protects against neurodegeneration in the cerebellum. Cell *130*, 548-562.

Chen, H.C., Vermulst, M., Wang, Y.E., Chomyn, A., Prolla, T.A., McCaffery, J.M., and Chan, D.C. (2010). Mitochondrial Fusion Is Required for mtDNA Stability in Skeletal Muscle and Tolerance of mtDNA Mutations. Cell *141*, 280-289.
Cohen, T., Levin, L., and Mishmar, D. (2016). Ancient Out-of-Africa Mitochondrial DNA Variants Associate with Distinct Mitochondrial Gene Expression Patterns. PLoS Genet *12*, e1006407.
Craven, L., Alston, C.L., Taylor, R.W., and Turnbull, D.M. (2017). Recent Advances in Mitochondrial Disease. Annu Rev Genomics Hum Genet *18*, 257-275.
F., K. (2015). Trim galore: A wrapper tool around Cutadapt and FastQC to consistently apply quality and adapter trimming to FastQ files.
Floros, V.I., Pyle, A., Dietmann, S., Wei, W., Tang, W.C.W., Irie, N., Payne, B., Capalbo, A., Noli, L., Coxhead, J., et al. (2018). Segregation of mitochondrial DNA heteroplasmy through a developmental genetic bottleneck in human embryos. Nat Cell Biol *20*, 144-151.
Gammage, P.A., Viscomi, C., Simard, M.L., Costa, A.S.H., Gaude, E., Powell, C.A., Van Haute, L., McCann, B., Rebelo-Guiomar, P., Cerutti, R., et al. (2018). Genome editing in mitochondria corrects a pathogenic mtDNA mutation in vivo. Nat Med *24*, 1691-1695.
Gilkerson, R.W., Schon, E.A., Hernandez, E., and Davidson, M.M. (2008). Mitochondrial nucleoids maintain genetic autonomy but allow for functional complementation. J Cell Biol *181*, 1117-1128.
Gitschlag, B.L., Kirby, C.S., Samuels, D.C., Gangula, R.D., Mallal, S.A., and Patel, M.R. (2016). Homeostatic responses regulate selfish mitochondrial genome dynamics in C. elegans. Cell metabolism *24*, 91-103.
Hahn, A., and Zuryn, S. (2019). The Cellular Mitochondrial Genome Landscape in Disease. Trends Cell Biol *29*, 227-240.
Kanazawa, T., Zappaterra, M.D., Hasegawa, A., Wright, A.P., Newman-Smith, E.D., Buttle, K.F., McDonald, K., Mannella, C.A., and van der Bliek, A.M. (2008). The C. elegans Opa1 homologue EAT-3 is essential for resistance to free radicals. PLoS genetics *4*, e1000022.
Kandul, N.P., Zhang, T., Hay, B.A., and Guo, M. (2016). Selective removal of deletion-bearing mitochondrial DNA in heteroplasmic Drosophila. Nature Communications *7*, 13100.
Klein, C.J., Kimmel, G.W., Pittock, S.J., Engelstad, J.E., Cunningham, J.M., Wu, Y.H., and Dyck, P.J. (2011). Large Kindred Evaluation of Mitofusin 2 Novel Mutation, Extremes of Neurologic Presentations, and Preserved Nerve Mitochondria. Arch Neurol-Chicago *68*, 1295-1302.
Kloss-Brandstatter, A., Pacher, D., Schonherr, S., Weissensteiner, H., Binna, R., Specht, G., and Kronenberg, F. (2011). HaploGrep: a fast and reliable algorithm for automatic classification of mitochondrial DNA haplogroups. Hum Mutat *32*, 25-32.
Li, H., and Durbin, R. (2009). Fast and accurate short read alignment with Burrows-Wheeler transform. Bioinformatics *25*, 1754-1760.
Li, H., Handsaker, B., Wysoker, A., Fennell, T., Ruan, J., Homer, N., Marth, G., Abecasis, G., Durbin, R., and Subgroup., G.P.D.P. (2009). The Sequence Alignment/Map format and SAMtools. Bioinformatics *25*, 2078-2079.
Liau, W.-S., Gonzalez-Serricchio, A.S., Deshommes, C., Chin, K., and LaMunyon, C.W. (2007). A persistent mitochondrial deletion reduces fitness and sperm performance in heteroplasmic populations of C. elegans. BMC genetics *8*, 8.
Livak, K.J., and Schmittgen, T.D. (2001). Analysis of relative gene expression data using real-time quantitative PCR and the 2(-Delta Delta C(T)) Method. Methods *25*, 402-408.
Malena, A., Loro, E., Di Re, M., Holt, I.J., and Vergani, L. (2009). Inhibition of mitochondrial fission favours mutant over wild-type mitochondrial DNA. Hum Mol Genet *18*, 3407-3416.

Mao, K., Wang, K., Liu, X., and Klionsky, D.J. (2013). The scaffold protein Atg11 recruits fission machinery to drive selective mitochondria degradation by autophagy. Dev Cell *26*, 9-18.
Nargund, A.M., Pellegrino, M.W., Fiorese, C.J., Baker, B.M., and Haynes, C.M. (2012). Mitochondrial import efficiency of ATFS-1 regulates mitochondrial UPR activation. Science *337*, 587-590.
Pang, W., Zhang, Y., Zhao, N., Darwiche, S.S., Fu, X., and Xiang, W. (2013). Low expression of Mfn2 is associated with mitochondrial damage and apoptosis in the placental villi of early unexplained miscarriage. Placenta *34*, 613-618.
Rebolledo-Jaramillo, B., Su, M.S.-W., Stoler, N., McElhoe, J.A., Dickins, B., Blankenberg, D., Korneliussen, T.S., Chiaromonte, F., Nielsen, R., and Holland, M.M. (2014). Maternal age effect and severe germ-line bottleneck in the inheritance of human mitochondrial DNA. Proceedings of the National Academy of Sciences *111*, 15474-15479.
Robinson, J.T., Thorvaldsdottir, H., Winckler, W., Guttman, M., Lander, E.S., Getz, G., and Mesirov, J.P. (2011). Integrative genomics viewer. Nat Biotechnol *29*, 24-26.
Schon, E.A., and Gilkerson, R.W. (2010). Functional complementation of mitochondrial DNAs: mobilizing mitochondrial genetics against dysfunction. Biochimica et Biophysica Acta (BBA)-General Subjects *1800*, 245-249.
Suen, D.F., Narendra, D.P., Tanaka, A., Manfredi, G., and Youle, R.J. (2010). Parkin overexpression selects against a deleterious mtDNA mutation in heteroplasmic cybrid cells. Proc Natl Acad Sci U S A *107*, 11835-11840.
Tsang, W.Y., and Lemire, B.D. (2002). Stable heteroplasmy but differential inheritance of a large mitochondrial DNA deletion in nematodes. Biochemistry and cell biology *80*, 645-654.
Twig, G., Elorza, A., Molina, A.J.A., Mohamed, H., Wikstrom, J.D., Walzer, G., Stiles, L., Haigh, S.E., Katz, S., Las, G., et al. (2008). Fission and selective fusion govern mitochondrial segregation and elimination by autophagy. Embo J *27*, 433-446.
Valenci, I., Yonai, L., Bar-Yaacov, D., Mishmar, D., and Ben-Zvi, A. (2015). Parkin modulates heteroplasmy of truncated mtDNA in Caenorhabditis elegans. Mitochondrion *20*, 64-70.
Verhoeven, K., Claeys, K.G., Zuchner, S., Schroder, J.M., Weis, J., Ceuterick, C., Jordanova, A., Nelis, E., De Vriendt, E., Van Hul, M., et al. (2006). MFN2 mutation distribution and genotype/phenotype correlation in Charcot-Marie-Tooth type 2. Brain *129*, 2093-2102.
Ye, K., Lu, J., Ma, F., Keinan, A., and Gu, Z. (2014). Extensive pathogenicity of mitochondrial heteroplasmy in healthy human individuals. Proceedings of the National Academy of Sciences *111*, 10654-10659.
Zuchner, S., Mersiyanova, I.V., Muglia, M., Bissar-Tadmouri, N., Rochelle, J., Dadali, E.L., Zappia, M., Nelis, E., Patitucci, A., Senderek, J., et al. (2004). Mutations in the mitochondrial GTPase mitofusin 2 cause Charcot-Marie-Tooth neuropathy type 2A. Nat Genet *36*, 449-451.

Figure legends

Figure 1: ΔmtDNA and *fzo-1(mut)* cannot co-exist. (A) Schematic representation of experimental setup, Heteroplasmic hermaphrodites (ΔmtDNA) were crossed with *fzo-1(mut)* males. Cross progeny F1 were allowed to self-propagate and single F2 (generation 1; G1) animals were isolated, allowed to lay eggs and their genotypes were determined. We then monitored heteroplasmic mutant or wild type *fzo-1* progeny over several generations (G2m-G4m and G2wt-G4wt, respectively). Heterozygous progeny was maintained to generate generation G1 without additional crosses. (B) The percent of hatched embryos of parental strains: N2(WT), ΔmtDNA and *fzo-1(mut)*, of *fzo-1(mut)* mutant cross progeny across generations (G1m-G4m) and of the stable cross line (>20 generations). (C) The percent of gravid adults six days after egg laying of parental strains: N2(WT), ΔmtDNA and *fzo-1(mut)*, and of mutant cross progeny across generations (G1m-G4m). (D) The percent of gravid adults of mutant cross progeny across generations (G1m-G4m) at the indicated times after egg laying. P values were calculated by comparison with *fzo-1(mut)* animals. (*) denotes P<0.05 and (**) denotes P<0.01.

Figure 2: ΔmtDNA levels are selectively eliminated in *fzo-1(mut)*;ΔmtDNA animals across generations. (A) The percent of ΔmtDNA determined in individual animals (n≥20) of the parental heteroplasmic strain ΔmtDNA, the *fzo-1(mut)* mutant cross-progeny strains (F1(ht), G1m-G4m) and the progeny of G4m animals crossed with *fzo-1(wt)*, (G4m->G6-8wt). (B) The percent of ΔmtDNA determined in individual animals (n≥20) of the *fzo-1(wt)* cross progeny strains (G1wt-G4wt). (C) The percent of ΔmtDNA determined in a population of animals of the stable cross lines (>20 generations). P values were calculated by comparison with *fzo-1(wt);*ΔmtDNA animals. (*) denotes P<0.05 and (**) denotes P<0.01.

Figure 3: ΔmtDNA molecules are selectively eliminated in two different developmental stages during the *C. elegans* life cycle. (A) The percent of ΔmtDNA in embryos and adults of the G2m-G3m generations. (B) The percent of ΔmtDNA in embryos and adults of the G2wt-G3wt generations. (C) The ratio of ΔmtDNA or +mtDNA levels in the gonad and soma of generation G2m adults P values were calculated by comparison with *fzo-1(mut)* G2 embryos. (*) denotes P<0.05.

Figure 4: A model depicting the selective removal of ΔmtDNA across generation in the *C. elegans* gonad. ΔmtDNA (red), intact mtDNA (black).

Table 1: Heteroplasmy in analyzed patient samples

Sample	mtDNA position	Heteroplasmy level	Best reads	Secondary reads
K_V13	16172	6.24	T	C
	310	1.59	T	C
	15880	1.19	A	G
K_V14	6899	10.59	G	A
	16172	10.08	T	C
	3447	1.91	A	C
	4665	1.88	G	A
	310	1.29	T	C
K_V17	16172	10.34	C	T
	6899	8.82	G	A
	310	1.06	T	C
K_VI9	152	9.93	T	C
	3492	4.26	A	C
	15515	2.94	A	G
	378	2.47	C	T
	3447	2.30	A	C
	3677	2.13	A	G
	310	1.60	T	C
	6764	1.26	G	A
	14882	1.23	A	G
	3475	1.17	A	C
Z_1007	13830	20.28	T	C
	13711	2.86	G	A
	13869	2.82	T	C
	13855	2.78	C	T
	13707	2.58	G	A
	14053	2.37	A	G
	13899	2.23	T	C
	14034	2.13	T	C
	13708	2.08	G	A
	14088	2.07	T	C
	13712	2.06	C	T
	14041	1.92	C	T
	13833	1.91	A	G
	14020	1.75	T	A
	13674	1.74	T	C
	14016	1.71	G	A
	14033	1.69	T	C
	14073	1.65	C	T
	14048	1.60	T	C
	14122	1.56	A	C
	13908	1.48	C	T
	13905	1.45	C	T
	14133	1.42	A	C

	13686	1.37	A	G
	13929	1.33	C	T
	13934	1.31	C	T
	13698	1.31	T	C
	13811	1.29	C	G
	13920	1.25	C	T
	13809	1.24	C	A
	14305	1.23	G	A
	13680	1.21	C	T
	13968	1.15	G	A
	14280	1.15	A	G
	14287	1.13	T	C
	13691	1.12	A	G
	13950	1.07	C	T
	14275	1.06	C	T
	14276	1.01	C	G
	13945	1.00	A	G
Z_1008	13830	35.00	T	C
	9722	2.16	T	C
	5368	1.22	C	G
Z_0106	13830	25.38	C	T
	310	1.08	T	C
N_SD1	4491	1.80	G	A
N_SD2	11963	1.37	G	A
	11812	1.31	G	A
	12007	1.29	G	A
	11914	1.22	G	A
	12013	1.14	A	G
	11887	1.02	G	A
N_SD3	5070	1.54	A	G

A.

P0: ♂ *fzo-1 (ht)* x ΔmtDNA ♀

F1: ♂ *fzo-1 (ht)*,ΔmtDNA

F2(G1): ♂ *fzo-1 (wt)*,ΔmtDNA → G2wt: *fzo-1 (wt)*,ΔmtDNA…

↻ ♂ *fzo-1 (ht)*,ΔmtDNA

♂ *fzo-1 (mut)*,ΔmtDNA → G2m: *fzo-1 (mut)*,ΔmtDNA…

B.

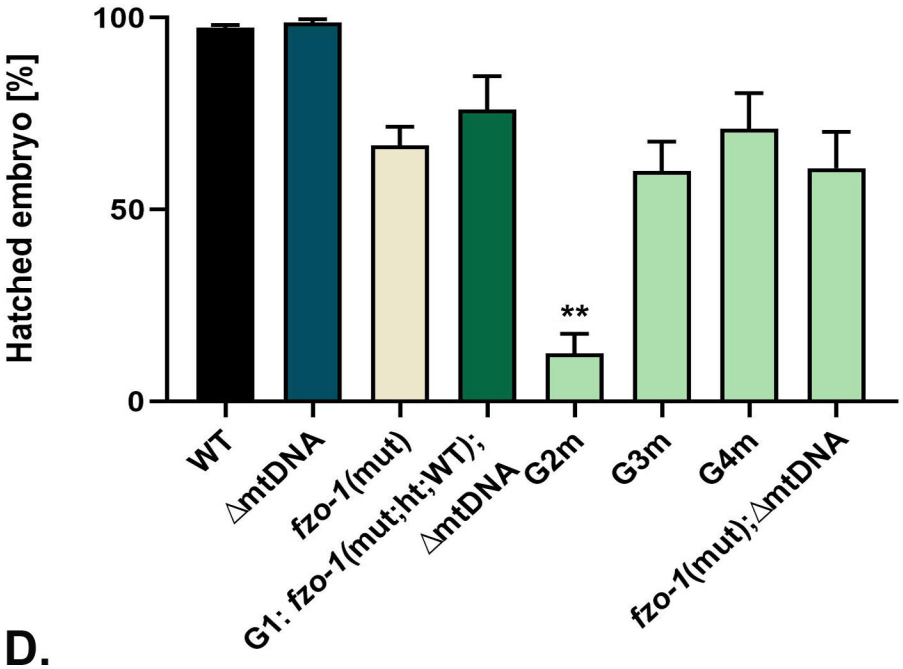

C.

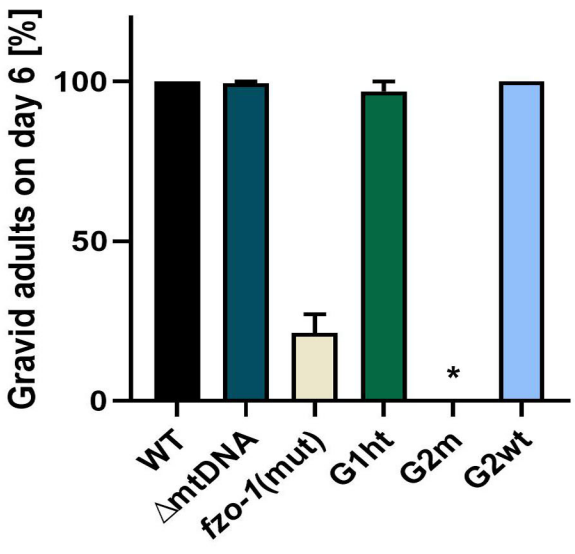

D.

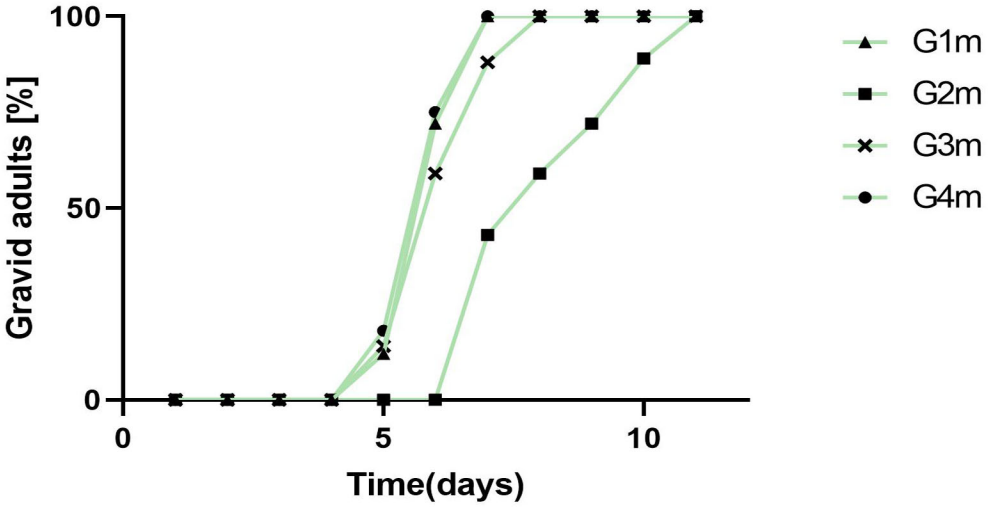

A.

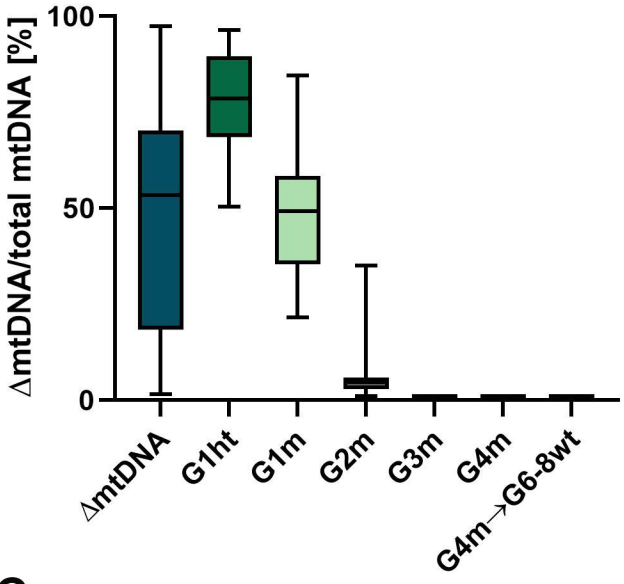
ΔmtDNA/total mtDNA [%]
100
50
0
ΔmtDNA
G1ht
G1m
G2m
G3m
G4m
G4m→G6-8wt

B.

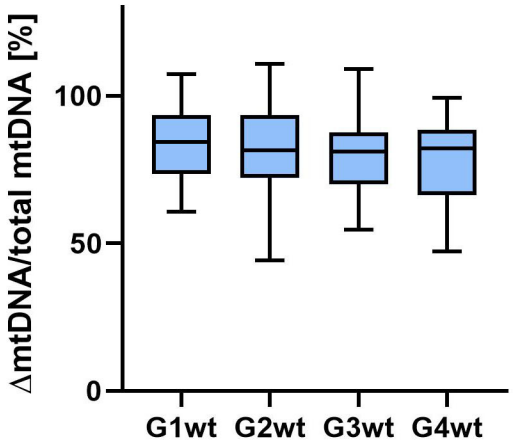
ΔmtDNA/total mtDNA [%]
100
50
0
G1wt
G2wt
G3wt
G4wt

C.

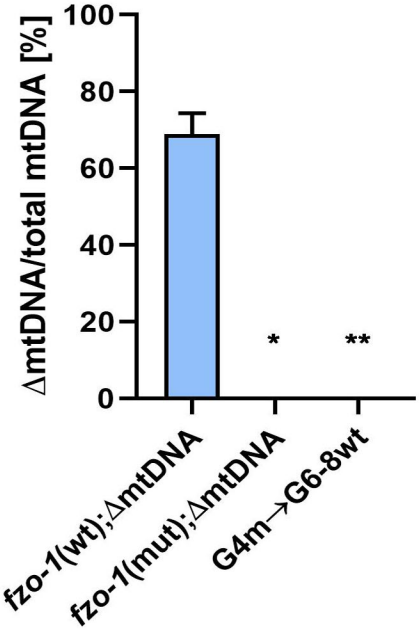
ΔmtDNA/total mtDNA [%]
100
80
60
40
20
0
*
**
fzo-1(wt);ΔmtDNA
fzo-1(mut);ΔmtDNA
G4m→G6-8wt

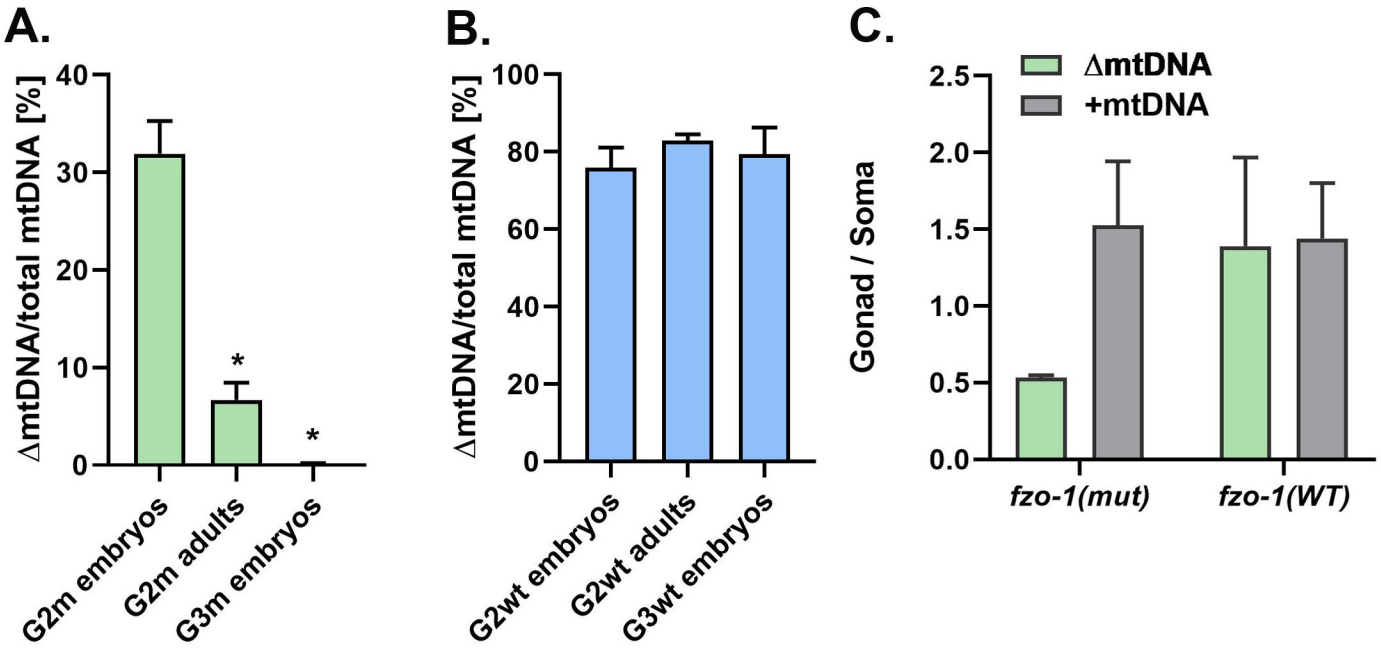
A.
ΔmtDNA/total mtDNA [%]
40
30
20
10
0
*
*
G2m embryos
G2m adults
G3m embryos
B.
ΔmtDNA/total mtDNA [%]
100
80
60
40
20
0
G2wt embryos
G2wt adults
G3wt embryos
C.
ΔmtDNA
+mtDNA
Gonad / Soma
2.5
2.0
1.5
1.0
0.5
0.0
fzo-1(mut)
fzo-1(WT)

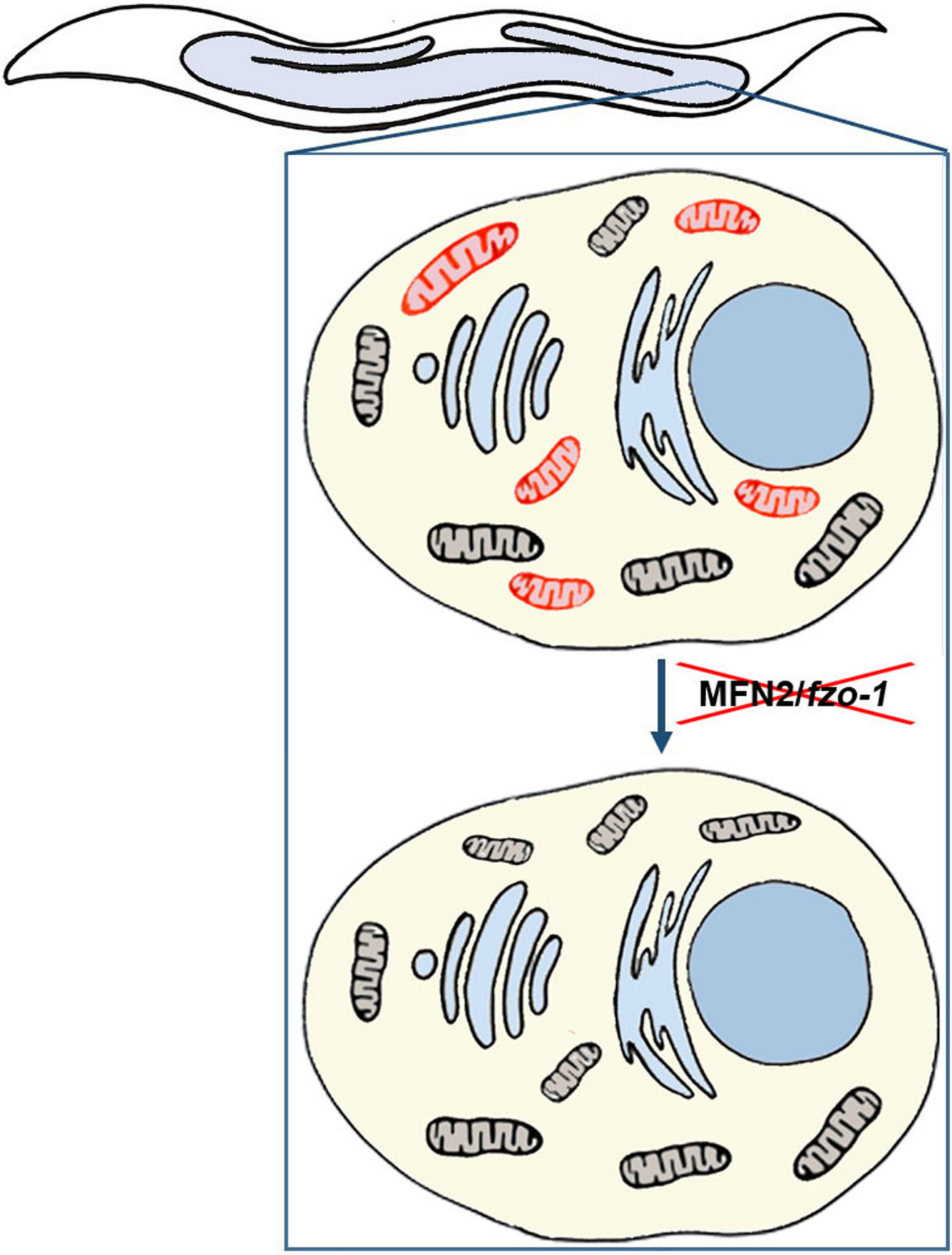
MFN2/fzo-1